



## Research Article

Academic Platform Journal of Natural Hazards and Disaster Management

4(2) 2023: 65-75, DOI: 10.52114/apjhad.1219257



# The September 26, 2019 Silivri Earthquake ( $M_w=5.6$ ), NW Türkiye

Murat Utkucu<sup>1,2\*</sup>, Fatih Uzunca<sup>3</sup>, Yelçin Utkucu<sup>4</sup>, Hatice Durmuş<sup>5</sup>, Serap Kırım<sup>3</sup>

<sup>1</sup> Department of Geophysics, Engineering Faculty, Sakarya University, Sakarya, Türkiye

<sup>2</sup> Disaster Management Application and Research Center, Sakarya University, Sakarya, Türkiye

<sup>3</sup> Institute of Natural Sciences, Sakarya University, Sakarya, Türkiye

<sup>4</sup> TOBB MTAL High School, Sakarya, Türkiye

<sup>5</sup> Geological Engineering Department, Engineering Faculty, Kütahya Dumlupınar University Kütahya, Türkiye

Received: / Accepted: 19-December-2022 / 22- December -2023

## Abstract

The September 26, 2019 Silivri earthquake ( $M_w=5.6-5.8$ ) occurred along the Northern Strand of the North Anatolian Fault Zone extending beneath the Marmara Sea. In the present study the teleseismic  $P$  waveforms and 20-year long background seismicity of the earthquake have been analyzed. Point-source inversion of the teleseismic  $P$  waveforms revealed that the earthquake was due to oblique faulting and released a seismic moment of  $3.2 \times 10^{17}$  Nm ( $M_w=5.6$ ). The frequency-magnitude distributions for the background seismicity have been calculated for 5-year long time windows after the 1999 İzmit earthquake. The considerable decrease of  $b$ -value of the frequency-magnitude distributions just before the 2019 Silivri earthquake has been interpreted as stress increase along the fault segments which provides a reasonable clue for the occurrence of the earthquake. The frequency-magnitude distribution for the 5 year-long time windows before the 2019 Silivri earthquake suggests a recurrence time interval of 168 years and occurrence probability of %16 within the next 30 years for a  $M_w=7.5$  earthquake.

**Key words:** The northern anatolian fault zone; The 26 September 2019 Silivri earthquake,  $B$ -value.

## 1. Introduction

The Marmara Region has been characterized by high seismic activity with tens of devastating large earthquakes in both historical (Figure 1a) and instrumental period (Figure 1b) [1, 2, 3, 4, 5]. The trench studies have confirmed the high seismic activity [6, 7, 8, 9, 10, 11]. The high seismic activity has been generated by the North Anatolian Fault Zone (NAFZ) which extends as three main fault strands, the Northern, Middle and Southern strands [12, 13, 14] (Figure 1a). As seen from Figure 1a the Northern fault strand has generated most of the large earthquakes. This fact indicates that the Northern fault strand has played major role in accommodating the deformation resulting from the regional plate kinematics, in accordance with GPS studies [15,16,17]. The fault segments of the Northern Strand have been indicated to be a seismic gap after the occurrence of the 1999 İzmit earthquake ( $M_w=7.5$ ) (Figure 1a) [18, 19, 20]. The largest city of Türkiye, İstanbul is located close to the seismic gap causing a high seismic risk. The September 26, 2019 Silivri earthquake ( $M_w=5.6-5.8$ ) occurred within the seismic gap along the Northern Strand (KOERI 2019; AFAD 2019; MTA 2019) (Figure 1a) and caused slight

\* Corresponding author e-mail: mutkucu@sakarya.edu.tr

structural damage and big fear among the population. Table 1 lists hypocentral and source parameters of the earthquake and indicates that the earthquake was produced by oblique faulting. In the present study teleseismic waveforms and seismicity around the earthquake will be analyzed in order to have an idea about seismotectonic meaning of the earthquake. Many seismicity studies carried out in the Marmara Region [21, 22, 23, 24, 25, 26].

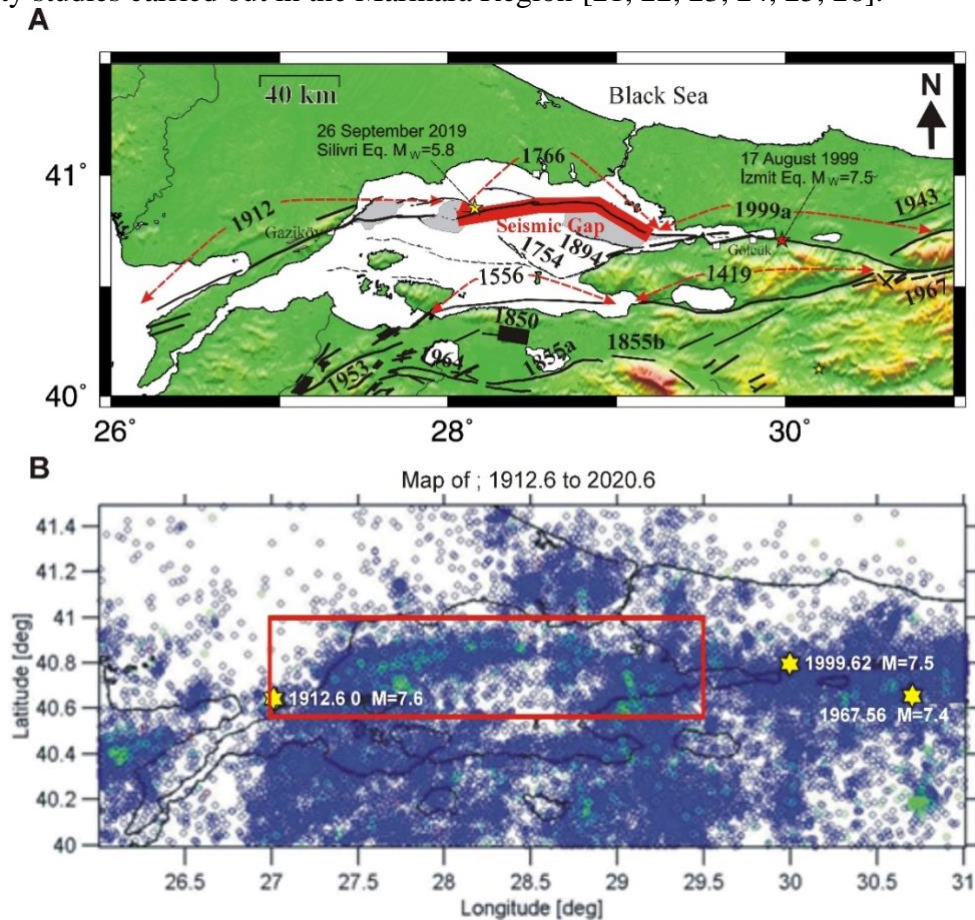


**Figure 1.** (a) The map demonstrating extent of the North Anatolian Fault Zone (NAFZ) and large historical earthquakes in the Marmara Region. The faults are compiled from [12, 13, 14] and the historical seismicity is taken from [2, 3]. The large rectangle encloses the areas in which the seismicity shown in Figures 3a and 4a have been recorded. Red thick line indicates fault segments that produced no large earthquake for the last hundred years along the Northern Strand and considered as seismic gaps. Red and yellow stars represent epicenters of the 1999 İzmit and the 2019 Silivri earthquakes, respectively. (b) Epicentral distribution of the all magnitude earthquakes after 1912 in the seismicity catalogue utilized in the study. Stars indicate the earthquake with  $M_w \geq 7.0$ .

## 2. Teleseismic Source Process

Teleseismic  $P$  waveforms of the 2019 Silivri earthquake recorded at 15 stations are inverted to investigate the source process and to obtain the source parameters. After corrected for the instrument responses and exclusion of the problematic recordings, the waveforms are bandpass filtered at corner frequencies from 0.01 to 0.35 Hz and resampled with 0.50 s time interval. Point-source inversion methodology developed by Kikuchi and Kanamori [26] is applied to the teleseismic  $P$  displacement waveforms, lengths of which are taken as 16 s. The earthquake rupture has been approximated by a vertical grid of  $5 \times 5$  point-sources along the strike and dip, respectively (Figure 2). The crustal structure given by Özer and Kenar [27] and a trapezoid source-rise time function with 1 s rise and fall and 3 s total duration are used in the calculations of the Green's functions. The rupture velocity is taken as 3.3 km/sec.

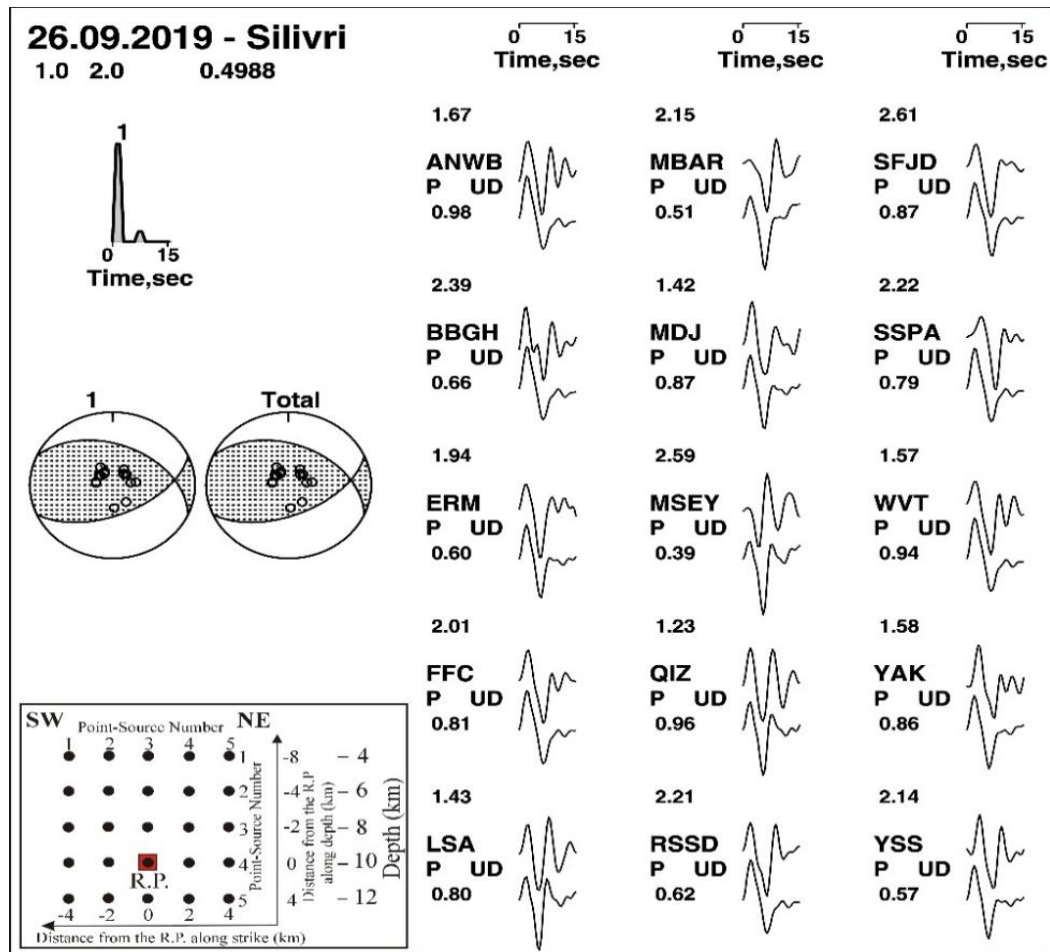


**Figure 2.** Teleseismic point-source analysis results of the September 26, 2019 Silivri earthquake. (Left) Source-time function, source mechanism and retrieved location of the single point-source. RP stands for the reference point which is taken as the hypocentral location in the analysis. (Right) Comparison of the observed waveforms (top) with synthetic waveforms (bottom) calculated for the point-source mechanism and location shown in the left.

**Table 1.** Lists hypocentral and source parameters of the 26 September 2019 Silivri earthquake and indicates that the earthquake was produced by oblique faulting.

	Longitude (degree)	Latitude (degree)	Depth (km)	Mw	Strike (degree)	Dip (degree)	Rake (degree)	Seismic Moment (10 <sup>18</sup> Nm)
<b>USGS</b>	28.150	40.904	8	5.71	86	64	123	0.4575
<b>NEIC</b>					210	42	42	
<b>Harvard</b>	28.25	40.86	12	5.7	273	49	144	0.404
<b>GCMT</b>					29	64	47	
<b>ISC</b>	28.1928	40.8901	12	5.7*				
<b>AFAD</b>	28.1928	40.8718	6.99	5.8	38	64	66	
					263	35	129	
<b>KOERI</b>	28.211	40.882	12,6	5.6	27	62	40	0.344
					276	55	145	
<b>This Study</b>					66	54	59	0.32
					294	44	128	

NEIC= National Earthquake Information Center; GCMT= Global Centroid Moment Tensor; Catalogue; ISC= International Seismological Centre; AFAD= Disaster and Emergency Management Presidency; KOERI= Kandilli Observatory and Earthquake Research Institute, \* Ms magnitude

The waveforms are satisfactorily fitted using single point-source located at the hypocentral depth (10 km). The results of the inversion are depicted in Figure 2 and calculated source parameters are listed in Table 1. Both hypocentral and source parameters of the earthquake suggest that the earthquake was due to oblique faulting with strike-slip and reverse faulting components. Adding relocation of the earthquake together with the detailed fault mapping suggest that the earthquake occurred on a secondary fault extending north of the main fault trace [28, 29, 30, 31]. The solution demonstrated in Figure 2 corresponds to a seismic moment of  $3.2 \times 10^{17}$  Nm ( $M_w=5.6$ ).

### 3. Seismicity Analysis

Gutenberg-Richter relation of the earthquake occurrences defines frequency-magnitude distribution (FMD) of earthquakes [32] and is given:

$$\log_{10} N = a - bM \quad (1)$$

where  $N$  represents cumulative number of earthquakes of size  $M$  and larger, and  $a$  and  $b$  are constant parameters. The parameter  $a$  is related with the level of seismicity while the  $b$ -value is an important seismotectonic parameter which has been pointed out to be inversely related to the crustal stresses and vary in the range 0.5-1.5 [33, 34]. In order to calculate  $a$  and  $b$ -values the Weighted Least Square method is utilized [35].

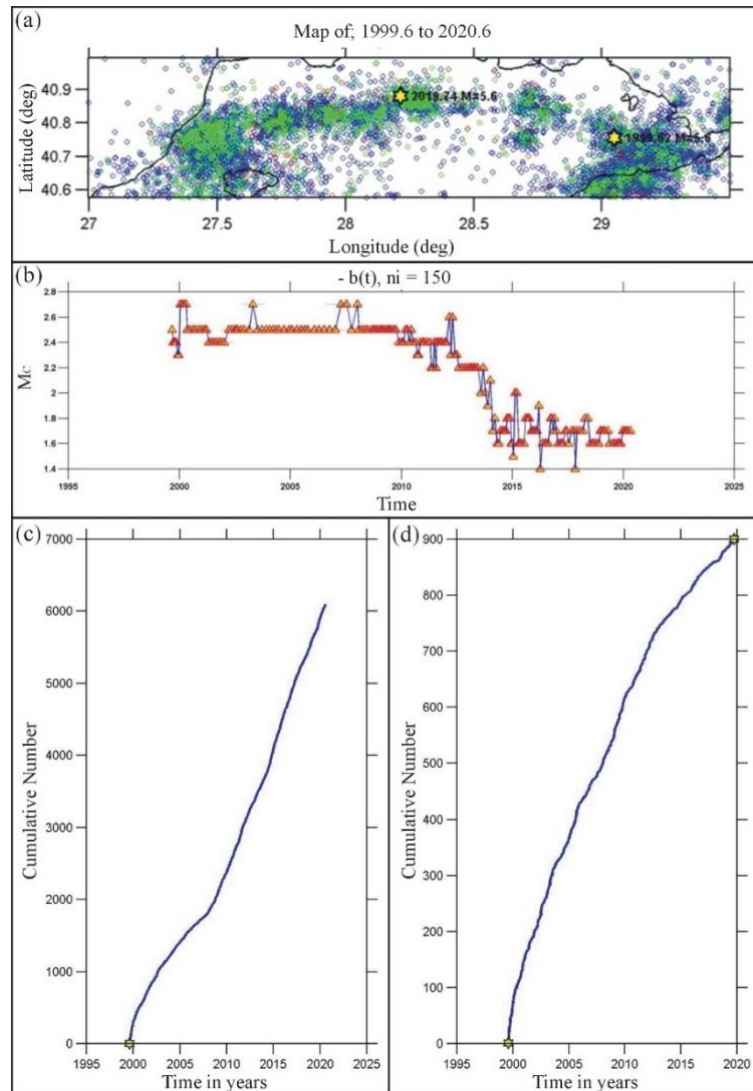
Following determination of the FMD relation from the seismicity recurrence time ( $T_r$ ) and occurrence possibility of an earthquake ( $R$ ) of targeted magnitude ( $M_{\text{targ}}$ ) in a defined future ( $t$ ) can be calculated by equations below

$$T_r = \frac{\Delta T}{10^{(a-bM_{\text{targ}})}} \quad (2)$$

$$R = 1 - e^{-N(M_{\text{targ}})t} \quad (3)$$

$$N(M_{\text{targ}}) = 10^{(a-bM_{\text{targ}})} \quad (4)$$

where  $\Delta T$  is the recording period of the seismicity [34, 36].  $N(M_{\text{targ}})$  corresponds annual number of occurrences of the targeted event. The *ZMAP* software is utilized for defining the FMD for the selected seismicity data [37]. Recurrence times and seismic risk are calculated manually. A homogenized catalogue that covers the time period from 1900 to October 2018 and is based on moment magnitude has been used in the seismicity analysis [5]. Kandilli Observatory and Earthquake Research Institute (KOERI) catalogue has been used to extend catalogue period until July 2020. The epicentral distribution of all magnitude seismicity from the combined catalogue after 1912 is demonstrated in Figure 1b.

The September 26, 2019 Silivri Earthquake ( $M_w=5.6$ ), NW Türkiye

**Figure 3.** (a) Declustered, all-magnitude seismicity along the Northern Strand after 1999 İzmit earthquake and calculated (b) magnitude of completeness ( $M_c$ ) time variations and (c) cumulative numbers of the seismicity shown. (d) Cumulative numbers of the seismicity for  $M_c \geq 2.8$ . Yellow stars represent the 1999 İzmit and the 2019 Silivri earthquakes. See Figure 4 for epicentral distribution of declustered  $M_c \geq 2.8$  seismicity and estimated Frequency-Magnitude distribution.

The seismicity after the 1999 İzmit earthquake and along the Northern Strand beneath the Marmara Sea (the seismicity in an area enclosed by a rectangle in Figure 1b) is used. Figure 3a shows the epicentral distribution of the selected seismology after declustering. Then temporal variations of  $M_c$  are calculated and result is shown Figure 3b. Figure 3c indicates cumulative numbers of earthquake for the seismicity shown in Figure 3a. The calculated magnitude of completeness time variations shown in Figure 3b for the declustered seismicity demonstrated in Figure 3a suggest that the seismicity is complete for  $M_w \geq 2.8$ . Figure 3d indicates cumulative numbers of earthquake for the declustered seismicity with  $M_w \geq 2.8$ . The calculated magnitude of completeness time variations and cumulative number plots for the all magnitude and  $M_w \geq 2.8$  seismicity shown in Figs 3b, 3c and 3d respectively, for the declustered seismicity illustrated in Figure 3a suggest that the seismicity data becomes more homogeneous after leaving only  $M \geq 2.8$  earthquakes in the catalogue. Therefore, the seismicity with  $M \geq 2.8$  is decided to be used in the later seismicity analysis. The epicentral distribution of the earthquakes in this catalogue is demonstrated Figure 4 along with the calculated FMD, which indicates a  $b$ -value of 1.06, a-value that virtually the same as global mean, 1.0.

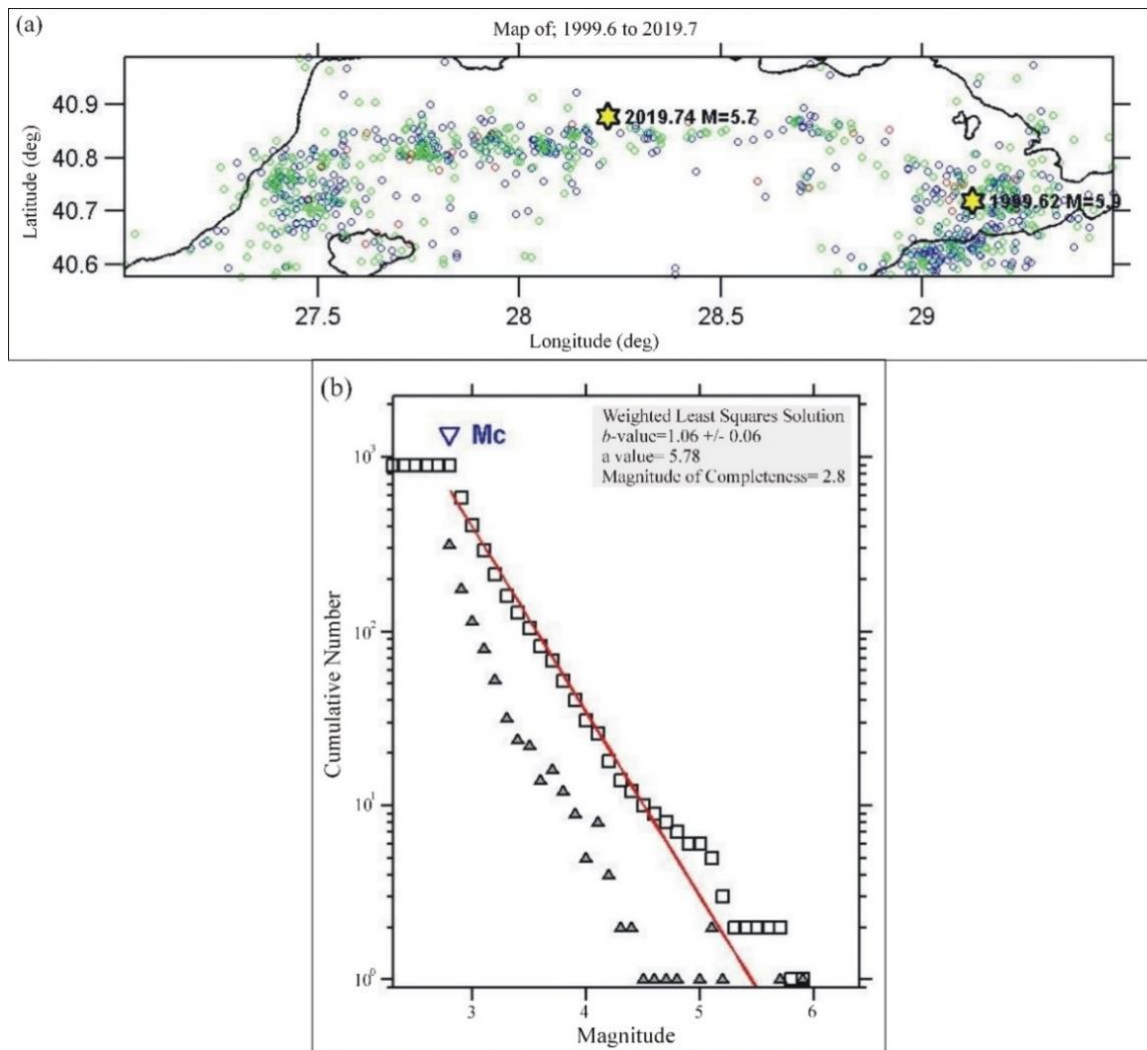


**Figure 4.** (a) Epicentral distribution of declustered  $M_c \geq 2.8$  seismicity. Yellow stars represent epicenters of the 1999 İzmit and the 2019 Silivri earthquakes. (b) Frequency-Magnitude distribution estimated for the declustered  $M_c \geq 2.8$  seismicity. The triangles and squares in (b) denote the discrete (non-cumulative) and the cumulative distributions of earthquakes, respectively.

#### 4. Discussion

Either source mechanism solution obtained in the study (Figure 2) and the previous solutions (Table 1) coincides with that the 2019 Silivri earthquake occurred along a secondary fault associated with a fault jog in the Central Basin of the Marmara Sea. In order to investigate if the background seismicity present a clue for occurrence of the 2019 Silivri earthquake the FMDs are estimated in 5-year time windows after the 1999 İzmit earthquake. The results are presented in Figure 5 which indicates considerable variations of  $b$ -value. Between 2004 and 2009  $b$ -value increased to 1.17 as compared with 5-year period just after the 1999 İzmit earthquake. Then it has gradually dropped 1.03 and 0.91 in the time intervals of 2009-2014 and 2014-2019, respectively. The significant drop in  $b$ -value suggests rise of crustal stresses along the fault segments lying beneath the Marmara Sea [28, 29] This provides a reasonable clue for the occurrence of the 2019 Silivri earthquake.

As indicated above fault segments of the NAFZ beneath the Marmara Sea comprise a seismic gap (Figure 1a). We have estimated earthquake recurrence times and seismic risks in the future for targeted magnitudes from the FMDs obtained in Figure 5. The computation results are listed

in Table 2. Notice that calculations suggest a recurrence time interval of 168 years and seismic risk or occurrence probability of %16 within the next 30 years for a  $M_w=7.5$  earthquake if the FMD of the 2014-2019 time-period with anomalously  $b$ -value is utilized. As for a  $M_w=7.0$  earthquake, calculations suggest a recurrence time interval of 59 years and occurrence probability of %40 within the next 30 years. The occurrence probabilities rise to %26 and %57 in the next 50 years for the same size earthquakes, respectively.

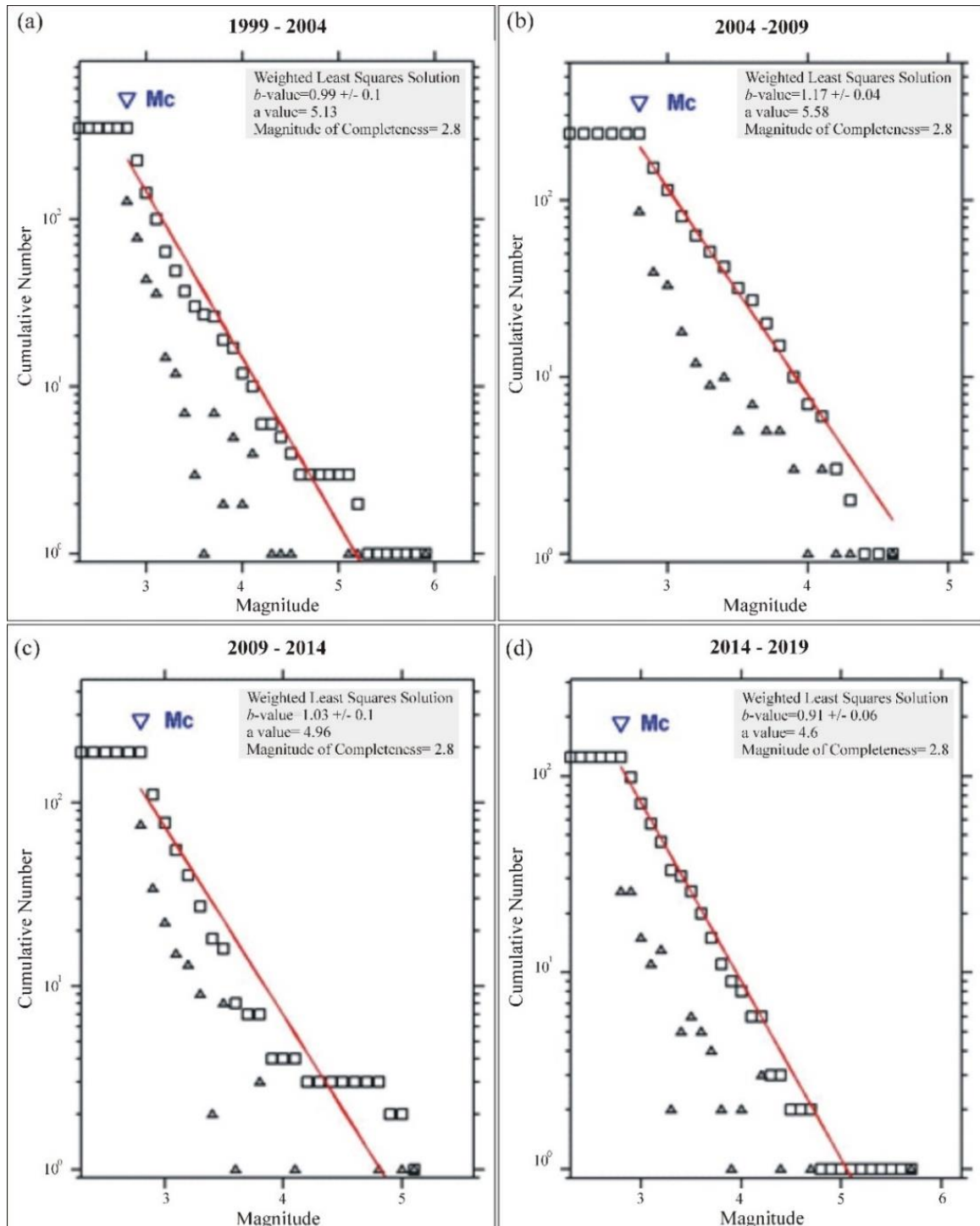


**Figure 5.** Estimated Frequency-Magnitude distributions of declustered  $M_c \geq 2.8$  seismicity after 1999 for the indicated 5 year-time intervals. See Figure 3d and Figure 4a for cumulative numbers and epicentral distribution of the seismicity, respectively. The triangles and squares denote the discrete (non-cumulative) and the cumulative distributions of earthquakes, respectively.

**Table 2.** Earthquake recurrence times ( $T_R$ ) and seismic risk ( $R$ ) or probability of earthquake occurrences for indicated magnitude of earthquakes along the fault segments of North Anatolian Fault Zone beneath the Marmara Sea. Calculations are based on the frequency-magnitude distributions (FMDs) obtained in the study (see Figures 4b and 5). The declustered seismicity along the fault segment after the 1999 İzmit are used in the FMD determinations (see Figure 4a)

	1999 - 2020	1999 - 2004	2004 - 2009	2009 - 2014	2014 - 2019	
<b>a-value</b>	5.78	5.13	5.58	4.96	4.6	
<b>b-value</b>	1.06±0.06	0.99±0.1	1.17±0.04	1.03±0.1	0.91±0.06	
<b>a-bM</b>	<b>M6.5</b>	-1.11	-1.305	-2.025	-1.305	-1.315
	<b>M7.0</b>	-1.64	-1.9	32.61	-2.25	-1.77
	<b>M7.5</b>	-2.17	-2.295	-3.195	-2.765	-2.225
<b>10<sup>a-bM</sup></b>	<b>M6.5</b>	0.07762	0.049	0.009	0.184	0.0484
	<b>M7.0</b>	0.0229	0.0156	0.0024	0.0056	0.0169
	<b>M7.5</b>	0.0067	0.005	0.0006	0.0017	0.0059
<b>T<sub>R</sub></b> <b>(year)</b>	<i>M6.5</i> 13	<i>M6.5</i> 20	<i>M6.5</i> 106	<i>M6.5</i> 5	<i>M6.5</i> 20	
	<i>M7.0</i> 44	<i>M7.0</i> 64	<i>M7.0</i> 407	<i>M7.0</i> 177	<i>M7.0</i> 59	
	<i>M7.5</i> 148	<i>M7.5</i> 197	<i>M7.5</i> 1567	<i>M7.5</i> 582	<i>M7.5</i> 168	
<b>R</b> <b>(percent in the next 30 years)</b>	<i>M6.5</i> 90	<i>M6.5</i> 77	<i>M6.5</i> 25	<i>M6.5</i> 42	<i>M6.5</i> 77	
	<i>M7.0</i> 50	<i>M7.0</i> 37	<i>M7.0</i> 7	<i>M7.0</i> 16	<i>M7.0</i> 40	
	<i>M7.5</i> 18	<i>M7.5</i> 14	<i>M7.5</i> 2	<i>M7.5</i> 5	<i>M7.5</i> 16	
<b>R</b> <b>(percent in the next 50 years)</b>	<i>M6.5</i> 98	<i>M6.5</i> 92	<i>M6.5</i> 38	<i>M6.5</i> 60	<i>M6.5</i> 91	
	<i>M7.0</i> 68	<i>M7.0</i> 54	<i>M7.0</i> 11	<i>M7.0</i> 25	<i>M7.0</i> 57	
	<i>M7.5</i> 29	<i>M7.5</i> 22	<i>M7.5</i> 3	<i>M7.5</i> 8	<i>M7.5</i> 26	

### 5. Conclusions

In the present study teleseismic P waveforms of the September 26, 2019 Silivri have been inverted for the source process and the background seismicity around the earthquake has been analyzed. The waveforms are fitted using single point-source located at the hypocentral depth (10 km) and calculated source parameters suggest that the earthquake was due to oblique faulting. The earthquake released a seismic moment of  $3.2 \times 10^{17}$  Nm ( $M_w=5.6$ ). The frequency-magnitude distributions (FMDs) for the background seismicity have been calculated in 5-year long time windows after the 1999 İzmit earthquake. The considerable decrease of *b*-value of the FMD for the time interval of 2014-2019 has been interpreted as stress increase along the fault segments which provides a reasonable clue for the occurrence of the 2019 Silivri earthquake. The FMD distribution for the seismicity in the 5-year time window before the 2019 Silivri earthquake suggest a recurrence time interval of 168 years and occurrence probability of %16 within the next 30 years for a  $M_w=7.5$  earthquake.

### Acknowledgements

This study was both funded by The Scientific and Technical Research Council of Türkiye (TÜBİTAK) (project number: 121Y271). Most of the figures were generated using Generic Mapping Tools (GMT) software available at (<http://gmt.soest.hawaii.edu/>) and a software package called ZMAP is used for mapping the *b*-value of FMD and TL value as a function of space. The data has been used the catalogues of Kandilli Observatory and Earthquake Research Institute (KOERI) of Turkey.

## Conflict of Interest

The authors declare no competing financial or personal interests that may appear and influence the work reported in this paper.

## Author Contributions

Murat Utkucu: Conceptualization, investigation, writing the original draft preparation, data curation, writing-review and editing; Fatih Uzunca: investigation, writing-review and editing, software, visualization, data curation; Yelçin Utkucu: Data processing, writing-review and editing; Hatice Durmuş: Software, investigation, writing-review and editing; Serap Kırım: writing-review and editing, visualization.

## References

- [1] A. Barka and K. Kadinsky-Cade, Strike-slip fault geometry in Turkey and its influence on earthquake activity, *Tectonics*, vol. 7, pp. 663-684, 1988.
- [2] N. Ambraseys. The seismic activity of the Marmara Sea Region over the last 2000 years, *Bull. Seism. Soc. Am.*, vol. 92, pp. 1-18, 2002.
- [3] N. Ambraseys, Earthquakes in the Mediterranean and Middle East: a multidisciplinary study of seismicity up to 1900, Cambridge University Press., ISBN: 978-0-521-87292-8, 2009.
- [4] D. Kalafat, Y. Günes, M. Kara, P. Deniz, K. Kekovalı, S. H. Kuleli, L. Gülen, M. Yılmaz, and N. Özel, A revised and extended earthquake catalogue for Turkey since 1900 (M4.0), Boğaziçi University, Kandilli Rasathanesi ve Deprem Araştırma Enstitüsü, Bebek-İstanbul, 553 pp., 2007.
- [5] O. Tan, A homogeneous earthquake catalogue for Turkey, *Nat. Hazards Earth Syst. Sci.*, vol. 21, pp. 2059–2073, 2021. <https://doi.org/10.5194/nhess-21-2059-2021>.
- [6] K. T. Rockwell, A. Barka, T. Dawson, H. S.Akyuz, K. Thorup, Paleoseismology of the Gazikoy-Saros segment of the North Antolia fault, Northwestern Turkey: Comparison of the historical and paleoseismic records, implications of regional seismic hazard, and models of earthquake recurrence, *Journal of Seismology* 5(3), 433-448. 2001. DOI:10.1023/A:1011435927983.
- [7] Y. Klinger, K. Sieh, E. Altunel, A. Akoglu, A. Barka, T. Dawson, T. Gonzalez, A. Meltzner and T. Rockwell, Paleoseismic Evidence of Characteristic Slip on the Western Segment of the North Anatolian Fault, Turkey. *Bull. Seism. Soc. Am.* 93, 2317-2332, 2003.
- [8] N. Palyvos, D. Pantosti, C. Zabcı and G. D'Addezio, Paleoseismological evidence of recent earthquakes on the 1967 Mudurnu Valley Earthquake segment of the North Anatolian Fault Zone, *Bulletin of the Seismological Society of America*, 97, 5, 1646-1661, 2007.
- [9] A. Kop, S. Özalp, H. Elmacı, M. Kara and T. Y. Duman, Active tectonic and palaeoseismological features of the western section of Mustafakemalpaşa Fault; Bursa, NW Anatolia, *Geodinamica Acta*, vol. 28, no. 4, pp. 363-378, 2016. <https://doi.org/10.1080/09853111.2016.1208525>
- [10] V. Özaksoy, H. Elmacı, Ö. Selim, K. Meryem and T.Y. Duman. Holocene activity of the Orhaneli Fault based on palaeoseismological data, Bursa, NW Anatolia, *Bull. Min. Res. Exp.*, 156: 1-16, 2018.

- [11] A. Kürçer, S. Özalp, E. Özdemir, Ç. U. Gündoğan and T. Y. Duman. Active tectonic and paleoseismologic characteristics of the Yenice-Gönen fault, NW Turkey, in light of the 18 March 1953 Yenice-Gönen Earthquake ( $M_s=7.2$ ), *MTA Dergisi*, 159, 29-63, 2019.
- [12] A. Barka and K. Kadinsky-Cade, Strike-slip fault geometry in Turkey and its influence on earthquake activity, *Tectonics*, vol. 7, pp. 663-684, 1988.
- [13] T. Armijo, B. Meyer, S. Navarro, G. King and A. Barka, Asymmetric slip partitioning in the Sea of Marmara pull-apart: a clue to propagation processes of the North Anatolian Fault, *Terra Nova*, vol. 14, pp. 80-86, 2002.
- [14] Ö. Emre, T. Y. Duman, S. Özalp, H. Elmacı, Ş. Olgun and F. Şaroğlu, Active fault map of Turkey with explanatory text, General Directorate of Mineral Research and Exploration Special Publication Series, 30, Ankara, Turkey, 2013.
- [15] F. Flerit, R. Armijo, G. C. P. King, B. Meyer and A. Barka, Slip partitioning in the Sea of Marmara pull-apart determined from GPS velocity vectors, *Geophys. J. Int.*, vol. 154, pp. 1-7, 2003.
- [16] R. Reilinger, S. McClusky, P. Vernant, S. Lawrence, S. Ergintav, et al. GPS constraints on continental deformation in the Africa-Arabia-Eurasia continental collision zone and implications for the dynamics of plate interactions, *J. Geophys. Res.*, Vol. 111, B05411, doi:10.1029/2005JB004051, 2006.
- [17] T. Parsons, S. Toda, R.S. Stein, A. Barka, J.H. Dieterich, Heightened odds of large earthquakes near İstanbul: An interaction-based probability calculation, *Science*, 288, 661-665, 2000.
- [18] A. Hubert-Ferrari, A. Barka, E. Jacques S. Nalbant, B. Meyer, R. Armijo, P. Tapponnier and G. C. P. King, Seismic hazard in the Marmara Sea region following the 17 August 1999 Izmit earthquake, *Nature*, 404, 262-27, 2000.
- [19] M. Utkucu, Z. Kanbur, Ö. Alptekin & F. Sünbül, Seismic behaviour of the North Anatolian Fault beneath the Sea of Marmara (NW Turkey): implications for earthquake recurrence times and future seismic hazard, *Natural Hazard*, 50(1), 45-71, 2009.
- [20] N. Pondard, R. Armijo, G.C.P. King, B. Meyer and F. Flerit, Fault interactions in the Sea of Marmara pull-apart (North Anatolian Fault): earthquake clustering and propagating earthquake sequences, *Geophysical Journal International*, 171, 3, 1185- 1197, 2007.
- [21] B. Akol, T. Bekler, Assessment of the statistical earthquake hazard parameters for NW Turkey, *Nat Hazards*, **68**, 837–853, <https://doi.org/10.1007/s11069-013-0659-1>, 2013
- [22] K. H. Çoban and N. L. Sayil, Different probabilistic models for earthquake occurrences along the North and East Anatolian fault zones, *Arabian Journal of Geosciences*, vol.13, no.18, 2020.
- [23] S. Öztürk, Characteristics of seismic activity in the Western, Central and Eastern parts of the North Anatolian Fault Zone, Turkey: Temporal and spatial analysis, *Acta Geophysica*, 59(2), 209–238, 2011.
- [24] N. L. Sayil, Long-term earthquake prediction in the Marmara region based on the regional time- and magnitude-predictable model, *Acta Geophysica*, vol.61, no.2, pp.338-356, 2013.
- [25] N. Sayıl, Evaluation of the seismicity for the Marmara region with statistical approaches, *Acta Geodaetica et Geophysica*, 49, 265–281, 2014.
- [26] M. Kikuchi, H. Kanamori, Inversion of complex body waves-III *Bulletin of the Seismological Society of America*, 81 (6), 2335-2350, 1991. <https://doi.org/10.1785/BSSA0810062335>
- [27] Ö. Kenar, M.N. Toksöz, Dispersion and Attenuation Properties of Surface Waves in Anatolia, *Jeofizik Dergisi*, 3(2), 1989.
- [28] R. Armijo, N. Pondard, B. Meyer, G. Uçarkus, B. Mercier de Lépinay, J. Malavieille, ... & K. Sarikavak, Submarine fault scarps in the Sea of Marmara pull-apart (North

- Anatolian Fault): Implications for seismic hazard in Istanbul, *Geochemistry, Geophysics, Geosystems*, 6(6), 2005.
- [29] P. Burnard, S. Bourlange, P. Henry, L. Geli, M. D. Tryon, B. Natal'in, A. M. C. Sengör, M. S. Özeren, M. N. Çagatay, Constraints on fluid origins and migration velocities along the Marmara Main Fault (Sea of Marmara, Turkey) using helium isotopes, *Earth and Planetary Science Letters*, Volumes 341-344, Pages 68-78, 2012.
- [30] B. Evangelia, A. Lomax, J. Tary, F. Klingelhoefer, V. Riboulot, S. Murphy, S. Monna, N. M. Özel, D. Kalafat, H. Saritas, G. Cifçi, N. Çagatay, L. Gasperini and L. Geli, An Alternative View of the Microseismicity along the Western Main Marmara Fault, *Bulletin of the Seismological Society of America*, Vol. 108, No. 5A, pp. 2650-2674, 2018.
- [31] Y. Yamamoto, D. Kalafat, A. Pinar, N. Takahashi, Z. Çoşkun, R. Polat, Y. Kaneda and H. Özener, Fault geometry beneath the western and Central Marmara Sea, Turkey, based on ocean bottom seismographic observations: Implications for future large earthquakes, *Tectonophysics*, Volume 791, <https://doi.org/10.1016/j.tecto.2020.228568>.
- [32] R. Gutenberg and C. F. Richter, Frequency of earthquakes in California, *Bull. Seismol. Soc. Am.*, vol. 34, pp. 185-188, 1944.
- [33] C.H. Scholz, Experimental Study of the Fracturing Process in Brittle Rock, *Journal of Geophysical Research*, 73(4), 1447-1454, 1968.
- [34] S. Wiemer and M. Wyss, Mapping the frequency-magnitude distribution in asperities: an improved technique to calculate recurrence times, *J. Geophys. Res.*, vol. 102, 15115-15128, 1997.
- [35] W. Menke, *Geophysical Data Analysis: Discrete Inverse Theory*, International Geophysics Series, Vol. 45, Academic Press, Inc., San Diego, California 92101, ISBN - 0-12-490921-3, 1989.
- [36] A. O. Öncel, M. Wyss, The major asperities of the 1999 Mw=7.4 İzmit earthquake defined by the microseismicity of the two decade before it, *Geophys. J. Int.* 143, 501-506, 2000.
- [37] S. Wiemer, A software package to analyse seismicity: ZMAP, *Seismological Research Letters*, 72(3), 373-382, 2001.



© 2023 by the authors. Submitted for possible open access publication under the terms and conditions of the Creative Commons Attribution (CC BY) License (<http://creativecommons.org/licenses/by/4.0/>).